Transport Coefficients of Isotactic Oligo- and Poly(methyl methacrylate)s in Dilute Solution

Nobuo Sawatari, Toshiki Konishi, Takenao Yoshizaki, and Hiromi Yamakawa*

Department of Polymer Chemistry, Kyoto University, Kyoto 606-01, Japan

Received September 28, 1994; Revised Manuscript Received November 10, 1994[⊗]

ABSTRACT: The intrinsic viscosity $[\eta]$ was determined for 25 samples of isotactic oligo- and poly(methyl methacrylate)s (i-PMMA), each with the fraction of racemic diads $f_r \simeq 0.01$, in the range of weight-average molecular weight M_w from 3.58×10^2 (trimer) to 1.71×10^6 in acetonitrile at 28.0 °C (Θ). The translational diffusion coefficient D was also determined from dynamic light scattering measurements for 12 of them in the range of M_w from 6.58×10^2 (hexamer) to 9.46×10^5 under the same solvent condition. It is found that $[\eta]$ is proportional to $M_w^{1/2}$ for $M_w \gtrsim 5 \times 10^4$ and its deviation from this asymptotic behavior is small even for smaller M_w, while D is inversely proportional to $M_w^{1/2}$ except for $M_w \lesssim 2 \times 10^3$. Such apparent Gaussian behavior of $[\eta]$ and D over a wide range of M_w is the result expected from that previously obtained for the mean-square radius of gyration $\langle S^2 \rangle$. From an analysis of these transport coefficients on the basis of the helical wormlike (HW) chain model, it is shown that the above M_w dependences of $[\eta]$ and D may be well explained by the HW theories with the values of the model parameters consistent with those previously determined from $\langle S^2 \rangle$. A comparison is also made of the present results for $[\eta]$ and D for i-PMMA with the previous ones for atactic (a-) PMMA with $f_r = 0.79$. This leads to the confirmation of the previous conclusion derived from $\langle S^2 \rangle$ concerning the f_r dependence of the chain stiffness and local chain conformation of PMMA. That is, the i-PMMA chain is of weaker helical nature than the a-PMMA chain that retains rather large and clearly distinguishable helical portions in dilute solution.

Introduction

Recently, we have been making an experimental study of dilute solution properties of poly(methyl methacrylate) (PMMA), giving attention to their dependence on its stereochemical composition.[1,2] Specifically, the mean-square radius of gyration[1] $\langle S^2 \rangle$ and scattering function[2] $P(k)$ have been determined for isotactic (i-) PMMA with the fraction of racemic diads $f_r \simeq 0.01$ in the unperturbed state, i.e., in acetonitrile at 28.0 °C (Θ), over a wide range of weight-average molecular weight M_w, including the oligomers with very low M_w, and then the results have been compared with those previously obtained for atactic (a-) PMMA with $f_r = 0.79$ in the same solvent at 44.0 °C (Θ).[3,4] In the present study, we further determine the steady-state transport coefficients, i.e., the intrinsic viscosity $[\eta]$ and translational diffusion coefficient D from viscosity and dynamic light scattering (DLS) measurements for the same i-PMMA samples in the same solvent (at Θ) as before[1,2] and compare the results with those previously[5,6] obtained for a-PMMA.

In the previous study[1] of $\langle S^2 \rangle$ for i-PMMA, it was found that the ratio $\langle S^2 \rangle / x_w$ as a function of the weight-average degree of polymerization x_w increases monotonically with increasing x_w and levels off to its asymptotic value 9.3_1 Å^2, differing from its behavior for a-PMMA,[3] for which it first increases for $x_w \lesssim 10$, then passes through a maximum at $x_w \simeq 50$, and finally approaches its asymptotic value 6.5_7 Å^2. On the basis of the helical wormlike (HW) chain,[7,8] this difference in the behavior of $\langle S^2 \rangle / x_w$ has been considered to arise from the difference in stiffness and local conformation between the i- and a-PMMA chains, and it has been concluded that the i-PMMA chain is of weaker helical nature[1,9] than the a-PMMA chain that retains rather large and clearly distinguishable helical portions in dilute solution. Because of such a difference in local chain conformation, the asymptotic value of $\langle S^2 \rangle / x_w$ is smaller for a-PMMA than for i-PMMA despite the fact that the chain stiffness is larger for the former than for the latter. The difference in the behavior of the Kratky plot of $P(k)$ between the i- and a-PMMA chains has also been well explained on the basis of the HW model.[2]

For a-PMMA, the double-logarithmic plot of $[\eta]$ against M_w deviates appreciably upward from its asymptotic straight line of slope $1/2$ with decreasing M_w for $M_w \lesssim 6 \times 10^4$, following an inverse S-shaped curve,[5] while the same plot of DM_w against M_w deviates downward from its asymptotic straight line of slope $1/2$ with decreasing M_w for $M_w \lesssim 5 \times 10^4$, following an S-shaped curve.[6] Such behavior of the transport coefficients for a-PMMA corresponds to the above-mentioned behavior of its $\langle S^2 \rangle / x_w$. As for i-PMMA, both plots may be expected to follow their respective asymptotic straight lines over a rather wide range of M_w, corresponding to the behavior of its $\langle S^2 \rangle / x_w$ above. The purpose of the present work is to confirm this expectation and examine whether the M_w dependences of $[\eta]$ and D for i-PMMA may be well explained by the HW theories[10,11] with values of the model parameters consistent with those previously[1] determined from $\langle S^2 \rangle$.

Finally, it is pertinent to make a remark on an experimental determination of the autocorrelation function of scattered light intensity $g^{(2)}(t)$ observed as a function of time t in the DLS measurements. Some effects of residual aggregates of solute molecules on $g^{(2)}(t)$ were observed for solutions of i-PMMA as well as for those of a-PMMA in acetonitrile, so that we have adopted the data acquisition procedure previously devised in the study of the latter[6] in order to remove the effects. We note that no appreciable dust effects were recognized as in the case of a-PMMA.[6]

Experimental Section

Materials. Most of the i-PMMA samples used in this work are the same as those used in the previous studies[1,2] of $\langle S^2 \rangle$

[⊗] Abstract published in *Advance ACS Abstracts,* February 1, 1995.

0024-9297/95/2228-1089$09.00/0

Table 1. Values of M_w, x_w, and M_w/M_n for Isotactic Oligo- and Poly(methyl methacrylate)s

sample	M_w	x_w	M_w/M_n
iOM3[a]	3.58×10^2	3	1.00
iOM4	4.58×10^2	4	1.00
iOM5	5.58×10^2	5	1.00
iOM6	6.58×10^2	6	1.00
iOM7	7.89×10^2	7.31	1.01
iOM10[b]	1.01×10^3	9.52	1.02
iOM18	1.79×10^3	17.3	1.10
iOM31	3.12×10^3	30.6	1.04
iOM71	7.07×10^3	70.1	1.05
iMM1	1.07×10^4	106	1.05
iMMc2	1.90×10^4	189	1.08
iMM2	2.57×10^4	256	1.07
iMM3	3.06×10^4	305	1.06
iMMc4	3.68×10^4	367	1.09
iMMc6	5.89×10^4	588	1.08
iMMc7	7.01×10^4	700	1.06
iMMc9	8.75×10^4	874	1.04
iMMc10	9.87×10^4	986	1.08
iMMc16	1.55×10^5	1550	1.08
iMMc30	3.13×10^5	3130	1.08
iMMc50	4.80×10^5	4800	1.08
iMMc60	5.82×10^5	5820	1.06
iMMc90	9.46×10^5	9460	1.09
iMMc100	9.61×10^5	9610	1.08
iMMc170	1.71×10^6	17100	1.09

[a] M_ws of iOM3 through iOM7 had been determined from ^{1}H NMR and GPC.[1] [b] M_ws of iOM70 through iMMc170 had been determined from LS in acetonitrile at 28.0 °C[1] except for iOM71 and iMMcx with x = 2, 6, 9, 10, 16, and 50, whose M_ws were similarly determined in this work.

and $P(k)$, i.e., the fractions separated by preparative gel permeation chromatography (GPC) or fractional precipitation from the original samples prepared by living anionic polymerization,[1] following the procedure of Ute et al.,[12] or from the commercial sample 9011-14-7 from Scientific Polymer Products, Inc. We also used some additional samples, iOM71 separated by fractional precipitation from an original sample previously prepared, and iMMc2, iMMc6, iMMc9, iMMc10, iMMc16, and iMMc50 separated similarly from the above commercial sample. The values of f_r for the additional samples were then found to be identical with those for the samples previously used, i.e., $f_r \simeq 0.01$. We note that the initiating chain-end group of the polymerized samples is a *tert*-butyl one and the other end is a hydrogen atom.

The values of M_w determined from ^{1}H NMR, analytical GPC, and (static) light scattering (LS) measurements (in acetonitrile at 28.0 °C), x_w, and the ratio of M_w to the number-average molecular weight M_n determined from analytical GPC are given in Table 1. As seen from the values of M_w/M_n, all the samples are sufficiently narrow in molecular weight distribution.

The solvent acetonitrile used for LS, viscosity, and DLS measurements was purified according to a standard procedure.

Light Scattering. LS measurements were carried out in acetonitrile at 28.0 °C to determine M_w of the seven additional samples iOM71, iMMc2, iMMc6, iMMc9, iMMc10, iMMc16, and iMMc50. A Fica 50 light scattering photometer was used for all the measurements with vertically polarized incident light of wavelength 436 nm. For a calibration of the apparatus, the intensity of light scattered from pure benzene was measured at a scattering angle of 90° at 25.0 °C, where the Rayleigh ratio $R_{Uu}(90°)$ of pure benzene was taken as 46.5×10^{-6} cm^{-1}. The depolarization ratio ϱ_u of pure benzene at 25.0 °C was determined to be 0.41 ± 0.01 by the method of Rubingh and Yu.[13] Scattering intensities were measured at five different concentrations and at scattering angles ranging from 30 to 150°. The data obtained were treated by the Berry square-root plot.[14] In the present case for which $M_w \gtrsim 7 \times 10^3$, corrections for the optical anisotropy were unnecessary since the degree of depolarization was negligibly small.

The most concentrated solution of each sample was prepared gravimetrically and made homogeneous by continuous stirring at 50 °C for 2 days. It was optically purified by filtration through a Teflon membrane of pore size 0.10–0.45 μm. The solutions of lower concentrations were obtained by successive dilution. The weight concentrations of the test solutions were converted to the polymer mass concentrations c by the use of the density of the solvent. We have used the value 0.144_9 cm^3/g of the refractive index increment $\partial n/\partial c$ previously determined[1] at 436 nm for i-PMMA samples with $M_w \gtrsim 3 \times 10^3$ in acetonitrile at 28.0 °C.

Viscosity. Viscosity measurements were carried out for all the samples listed in Table 1 in acetonitrile at 28.0 °C (Θ). For the measurements, we used conventional capillary and four-bulb spiral capillary viscometers of the Ubbelohde type. The flow time was measured to a precision of 0.1 s, keeping the difference between those of the solvent and solution larger than 20 s. The test solutions were maintained at a constant temperature within ±0.005 °C during the measurements. Density corrections were made in the calculations of the concentration c and also of the relative viscosity η_r from the flow times of the solution and solvent. The densities of the solvent and solution were measured with a pycnometer of the Lipkin–Davison type. The data obtained for the specific viscosity η_{sp} and η_r were treated as usual by the Huggins and Fuoss–Mead plots to determine $[\eta]$.

Dynamic Light Scattering. DLS measurements were carried out to determine D for 12 samples in acetonitrile at 28.0 °C (Θ) by the use of a Brookhaven Instruments Model BI-200SM light scattering goniometer with vertically polarized incident light of 488 nm wavelength from a Spectra-Physics Model 2020 argon ion laser equipped with a Model 583 temperature-stabilized etalon for single-frequency-mode operation. The photomultiplier tube used was EMI 9863B/350, the output from which was processed by a Brookhaven Instruments Model BI2030AT autocorrelator with 264 channels. (An electric shutter was attached to the original detector alignment in order to monitor the dark count automatically.[15]) The normalized autocorrelation function $g^{(2)}(t)$ of scattered light intensity $I(t)$ at time t was measured at four or five concentrations and at scattering angles θ ranging from 15 to 35°. All the test solutions were prepared in the same manner as in the case of LS measurements. However, the concentrations c of the solutions of the oligomer samples with $M_w \lesssim 2 \times 10^3$ were calculated by the use of the densities of the solutions instead of the solvent.

As mentioned in the Introduction, $g^{(2)}(t)$ for each solution was measured by the use of the data acquisition procedure previously[6] introduced in order to remove possible effects of residual aggregates of the solute molecules. In principle, the procedure consists of measuring successively a large number of sets of 264 values of $g^{(2)}(j\tau)$ with τ the sampling time (j = 1, 2, ..., 264), with the measurement for each set being made during 20 s. Only those sets of values which are free of such effects are then accumulated.

From the data for $g^{(2)}(t)$ thus determined at finite concentrations c, we determine D at an infinitely long time[16] at infinite dilution in the same manner as that used in the previous studies.[6,11,15,16] At small c, the plot of $(^1/_2)\ln[g^{(2)}(t) - 1]$ against t in general follows a straight line represented by

$$(^1/_2)\ln[g^{(2)}(t) - 1] = \text{const} - At \qquad (1)$$

with A the slope for such large t that all the internal motions of solute polymer chains have relaxed away.[16] As an example, $(^1/_2)\ln[g^{(2)}(t) - 1]$ at $\theta = 18°$ is plotted against t in Figure 1 for the sample iMMc90 in acetonitrile at 28.0 °C at $c = 1.26 \times 10^{-3}$ g/cm^3. It is seen that the data points obtained by the above-mentioned procedure follow a straight line (although invisible behind them), so that the slope A may be determined with sufficient accuracy.

With the slope A evaluated from the plot, we may determine the apparent diffusion coefficient $D^{(LS)}(c)$ at finite c from

$$D^{(LS)}(c) = \lim_{k \to 0} A/k^2 \qquad (2)$$

where k is the magnitude of the scattering vector and is given

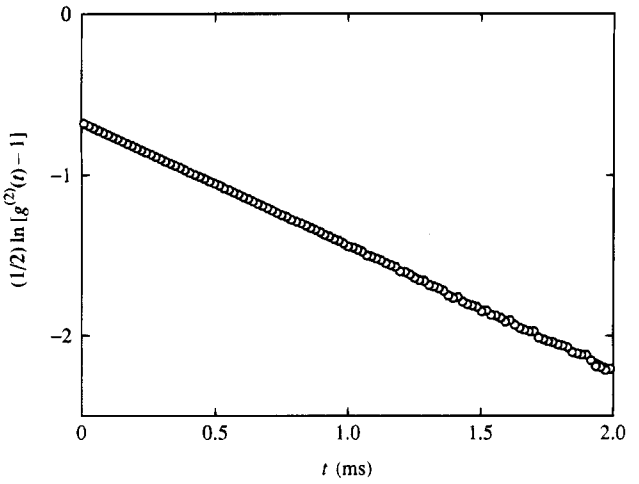

Figure 1. Plot of $(1/2)\ln[g^{(2)}(t) - 1]$ at $\theta = 18°$ against t for the i-PMMA sample iMMc90 in acetonitrile at 28.0 °C at $c = 1.26 \times 10^{-3}$ g/cm^3.

Table 2. Results of Viscometry on Isotactic Oligo- and Poly(methyl methacrylate)s in Acetonitrile at 28.0 °C

sample	$[\eta]$, dL/g	k'	sample	$[\eta]$, dL/g	k'
iOM3	0.0157	1.34	iMMc4	0.178	0.56
iOM4	0.0178	1.35	iMMc6	0.217	0.72
iOM5	0.0199	1.22	iMMc7	0.241	0.57
iOM6	0.0219	1.05	iMMc9	0.277	0.61
iOM7	0.0234	1.13	iMMc10	0.293	0.57
iOM10	0.0267	0.84	iMMc16	0.367	0.59
iOM18	0.0348	0.85	iMMc30	0.540	0.62
iOM31	0.0480	0.84	iMMc50	0.656	0.65
iOM71	0.0757	0.67	iMMc60	0.716	0.70
iMM1	0.0925	0.62	iMMc90	0.936	0.70
iMMc2	0.118	0.62	iMMc100	0.926	0.66
iMM2	0.138	0.60	iMMc170	1.26	0.70
iMM3	0.160	0.63			

by

$$k = (4\pi/\tilde{\lambda}) \sin(\theta/2) \tag{3}$$

with $\tilde{\lambda}$ the wavelength of the incident light in the solvent. At sufficiently small c, $D^{(LS)}(c)$ may be expanded as

$$D^{(LS)}(c) = D^{(LS)}(0)(1 + k_D^{(LS)}c + ...) \tag{4}$$

so that the desired $D = D(\infty)$ (at an infinitely long time) may be determined from extrapolation of $D^{(LS)}(c)$ to $c = 0$ as

$$D = D^{(LS)}(0) \tag{5}$$

The values of the refractive index at a wavelength of 488 nm and the viscosity coefficient η_0 of the pure solvent acetonitrile at 28.0 °C are 1.344 and 0.331 cP, respectively.

Results

Intrinsic Viscosity $[\eta]$. Intrinsic viscosity data for all the i-PMMA samples in acetonitrile at 28.0 °C are summarized in Table 2 along with the values of the Huggins coefficient k'. As M_w is decreased, k' first decreases from its asymptotic value ca. 0.7 in the limit of $M_w \to \infty$ to ca. 0.6 for $M_w \gtrsim 10^4$ and then increases for smaller M_w. Thus, k' as a function of M_w takes a minimum for i-PMMA as well as for a-PMMA in acetonitrile at Θ,[3] but we note that its asymptotic value for the former is appreciably smaller than the corresponding value ca. 1.1 for the latter.[4]

In Figure 2, the present data (unfilled circles) for $[\eta]$ (in dL/g) for i-PMMA in acetonitrile at 28.0 °C (Θ) are double-logarithmically plotted against M_w. The solid curve connects the data points smoothly, and the dotted line indicates its asymptotic straight line of slope $1/2$. They follow this straight line for $M_w \gtrsim 5 \times 10^4$ anddeviate only slightly downward from it with decreasing M_w for smaller M_w. The figure also includes the data (filled circles) obtained by Krause and Cohn-Ginsberg[17] for i-PMMA in acetonitrile at 27.6 °C. For their samples, however, we must note that the molecular weights are the viscosity-average ones determined in acetone at 30 °C, that those may be considered to have f_r equal to 0.1−0.2 and therefore somewhat larger than the value 0.01 for our samples, and that the Θ temperature determined in acetonitrile is 27.6 °C, which value is in rather good agreement with our value 28.0 °C. Thus the difference between our and their data for $[\eta]$ may be regarded as arising from the difference in f_r between our and their i-PMMA samples.

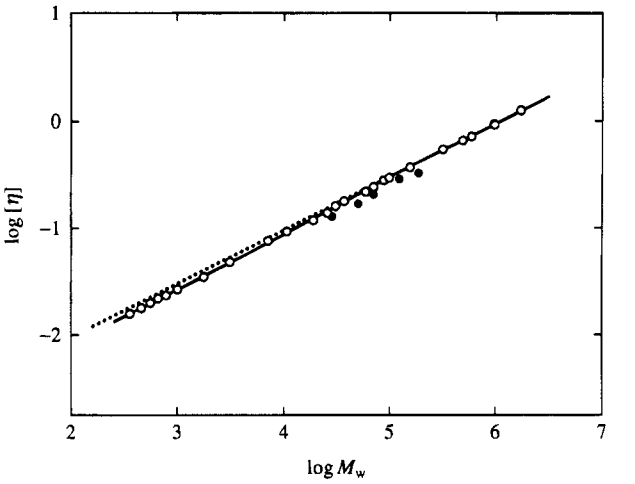

Figure 2. Double-logarithmic plots of $[\eta]$ (in dL/g) against M_w for i-PMMA in acetonitrile at 28.0 °C: (○) present data; (●) data by Krause and Cohn-Ginsberg (obtained at 27.6 °C).[17] The solid curve connects the data points smoothly and the dotted straight line has a slope of 0.5.

Translational Diffusion Coefficient D. In the range of k (or θ) where the DLS measurements were carried out, the ratio A/k^2 was independent of k within experimental error for all the test solutions, although we do not show the results. Then $D^{(LS)}(c)$ for each solution was determined as the mean of the observed values of A/k^2. Figure 3 shows plots of $D^{(LS)}(c)$ thus obtained against c for the 12 i-PMMA samples indicated in acetonitrile at 28.0 °C. As seen from the figure, the data points for each sample follow a straight line, and therefore $D^{(LS)}(0)$ (= D) and $k_D^{(LS)}$ may be determined from the ordinate intercept and slope, respectively. In Table 3 are given the values of D and $k_D^{(LS)}$ thus obtained.

Figure 4 shows double-logarithmic plots of $\eta_0 D M_w / k_B T$ (in cm^{-1}) against M_w, where k_B is the Boltzmann constant and T is the absolute temperature. (Note that the quantity $\eta_0 D M_w / k_B T$ is proportional to the sedimentation coefficient.) The solid curve connects the data points smoothly, and the dotted line indicates its asymptotic straight line of slope $1/2$. They are seen to follow this straight line except for $M_w \lesssim 2 \times 10^3$.

Discussion

Analysis of $[\eta]$ on the Basis of the HW Model. We first analyze the data for $[\eta]$ as usual on the basis of the HW touched-bead model.[10] The HW chain itself[7,8] may be described in terms of the four basic model

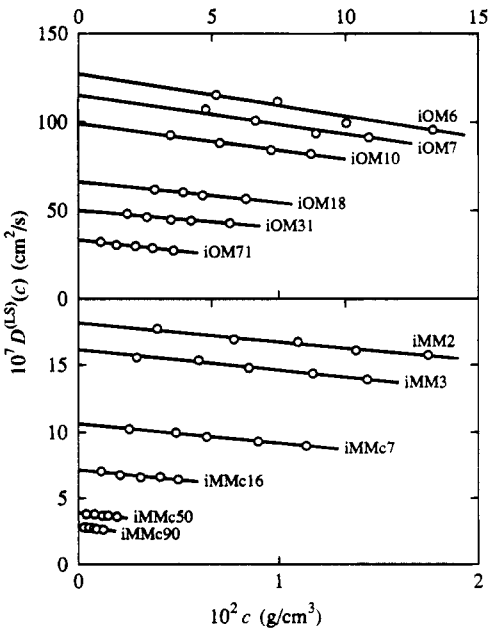

Figure 3. Plots of $D^{(LS)}(c)$ against c for the i-PMMA samples indicated in acetonitrile at 28.0 °C.

Table 3. Results of DLS Measurements on Isotactic Oligo- and Poly(methyl methacrylate)s in Acetonitrile at 28.0 °C

sample	10^7D, cm^2/s	$k_D^{(LS)}$, cm^3/g
iOM6	127	-1.9
iOM7	115	-1.9
iOM10	99.0	-2.0
iOM18	66.1	-2.4
iOM31	49.9	-2.6
iOM71	33.0	-4.9
iMM2	18.2	-7.8
iMM3	16.2	-9.8
iMMc7	10.6	-13.7
iMMc16	7.16	-21.3
iMMc50	3.91	-42.5
iMMc90	2.87	-65.5

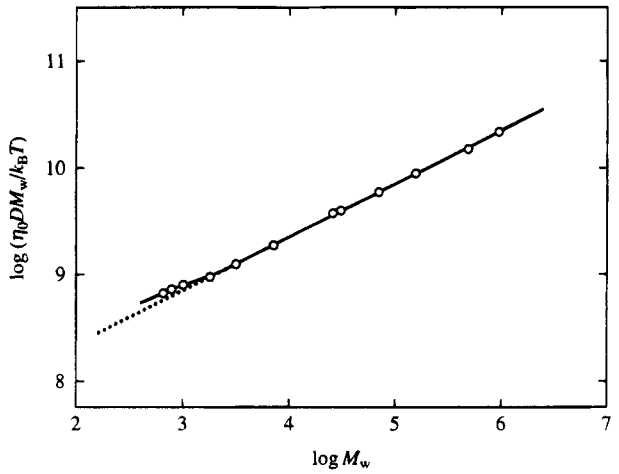

Figure 4. Double-logarithmic plots of $\eta_0 DM_w/k_BT$ (in cm^{-1}) against M_w for i-PMMA in acetonitrile at 28.0 °C. The solid curve connects the data points smoothly and the dotted straight line has a slope of 0.5.

parameters: the differential-geometrical curvature κ_0 and torsion τ_0 of its characteristic helix taken at the minimum zero of its elastic energy, the static stiffness parameter λ^{-1}, and the shift factor M_L as defined as the molecular weight per unit contour length. For the touched-bead model chain of total contour length $L = Nd_b$ with N the number of beads in the chain and d_b

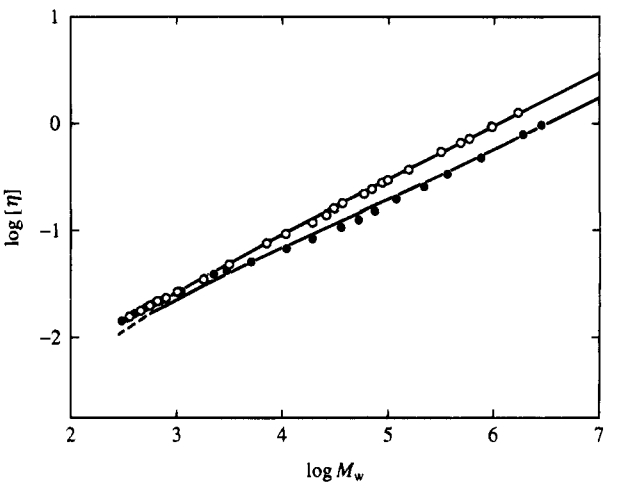

Figure 5. Double-logarithmic plots of $[\eta]$ (in dL/g) against M_w for PMMA in acetonitrile: (○) present data for i-PMMA at 28.0 °C; (●) previous data for a-PMMA at 44.0 °C.[5] The solid curves represent the respective best-fit HW theoretical values for $N \geq 2$, with the dashed line segments connecting the respective values for $N = 1$ and 2.

the diameter of the bead, $[\eta]$ may be written in the form[10]

$$[\eta] = (1/\lambda^2 M_L) f_\eta(\lambda L; \lambda^{-1}\kappa_0, \lambda^{-1}\tau_0, \lambda d_b) \quad (6)$$

where the function f_η is defined by

$$f_\eta(\lambda L) = \lambda^{-1} M_L [\bar{\eta}] \quad (7)$$

with $[\bar{\eta}]$ being the $[\eta]$ measured in units of $(\lambda^{-1})^3$ and being given by eq 15 with eqs 17 and 27 of ref 10. It satisfies the following asymptotic relation

$$\lim_{\lambda L \to \infty} f_\eta(\lambda L)/(\lambda L)^{1/2} = c_\infty^{3/2} \Phi_\infty \quad (8)$$

where

$$c_\infty = \frac{4 + (\lambda^{-1}\tau_0)^2}{4 + (\lambda^{-1}\kappa_0)^2 + (\lambda^{-1}\tau_0)^2} \quad (9)$$

and Φ_∞ denotes the (theoretical) coil-limiting value of the Flory–Fox factor $\Phi = M[\eta]/(6\langle S^2\rangle)^{3/2}$ with M the molecular weight (in the limit of $\lambda L \to \infty$) and is equal to 2.870×10^{23} mol^{-1} (for the unperturbed chain).

The basic equations required for an analysis of the data may then be written as

$$\log[\eta] = \log f_\eta(\lambda L) - \log(\lambda^2 M_L) \quad (10)$$

$$\log M_w = \log(\lambda L) + \log(\lambda^{-1} M_L) \quad (11)$$

Thus the quantities $\lambda^2 M_L$ and $\lambda^{-1} M_L$ (and therefore λ^{-1} and M_L) may be estimated from a best fit of double-logarithmic plots of the theoretical f_η against λL for properly chosen values of $\lambda^{-1}\kappa_0$, $\lambda^{-1}\tau_0$, and λd_b to that of the observed $[\eta]$ against M_w, so that we may determine $\lambda^{-1}\kappa_0$, $\lambda^{-1}\tau_0$, λ^{-1}, M_L, and d_b.

In Figure 5, the present data (unfilled circles) for $[\eta]$ (in dL/g) for i-PMMA in acetonitrile at 28.0 °C are double-logarithmically plotted against M_w, and the solid curve for them represents the best-fit theoretical values calculated for $N \geq 2$ from eq 6 with $\lambda^{-1}\kappa_0 = 2.5$, $\lambda^{-1}\tau_0 = 2.0$, $\lambda d_b = 0.25$, $\log(\lambda^2 M_L) = -1.44$, and $\log(\lambda^{-1} M_L) =$

Table 4. Values of the HW Model Parameters for Poly(methyl methacrylate) in Acetonitrile

f_r	temp, °C	$\lambda^{-1}\kappa_0$	$\lambda^{-1}\tau_0$	λ^{-1}, Å	M_L, Å^{-1}	d_b, Å	obsd quantity
0.01	28.0	2.5	2.0	32.6	38.6	8.2	$[\eta]$
		(2.5)	(2.0)	45.5	33.0	9.1	D
		2.5	1.3	38.0	32.5		$\langle S^2\rangle$[a]
0.79	44.0	4.5	2.0	45.0	38.6	7.2	$[\eta]$[b]
		(4.5)	(2.0)	65.0	35.0	9.0	D[c]
		4.0	1.1	57.9	36.3		$\langle S^2\rangle$[d]

[a] See ref 1. [b] See ref 5. [c] See ref 6. [d] See ref 3.

3.10, the dashed line segment connecting those values for $N = 1$ and 2. (The dashed line segment is invisible behind the data points.) The agreement between theory and experiment is seen to be good. The values of the HW model parameters thus determined are listed in the first row of Table 4. In the third row there are also given the values of the model parameters (except for d_b) previously[1] determined from $\langle S^2\rangle$. The value of $\lambda^{-1}\tau_0$ determined from $[\eta]$ is somewhat larger than that from $\langle S^2\rangle$, but this does not change the previous conclusion about the helical nature of the i-PMMA chain. The differences between the values of the model parameters λ^{-1} and also M_L determined from $[\eta]$ and $\langle S^2\rangle$ may be regarded as arising from the disagreement between the theoretical and experimental values of Φ_∞.[15] Thus the two sets of parameter values from the two different properties may rather be considered to be consistent with each other.

Analysis of D on the Basis of the HW Model. The quantity $\eta_0 DM_w/k_BT$ for the same HW touched-bead model as above may be written in the form[11]

$$\eta_0 DM_w/k_BT = (M_L/3\pi)f_D(\lambda L;\lambda^{-1}\kappa_0,\lambda^{-1}\tau_0,\lambda d_b) \quad (12)$$

where the function f_D is given by eq 6 of ref 11 and may be evaluated numerically by the use of the interpolation formula for the mean reciprocal end-to-end distance of the chain as given in the Appendix of ref 18. The function f_D satisfies the following asymptotic relation

$$\lim_{\lambda L\to\infty} f_D(\lambda L)/(\lambda L)^{1/2} = (\sqrt{6}/2)c_\infty^{-1/2}\varrho_\infty \quad (13)$$

where c_∞ is given by eq 9 and ϱ_∞ denotes the (theoretical) coil-limiting value of the ratio ϱ of the root-mean-square radius of gyration $\langle S^2\rangle^{1/2}$ to the hydrodynamic radius $R_H \equiv k_BT/6\pi\eta_0 D$ and is equal to the Kirkwood value 1.505 (for the unperturbed chain).[19]

The basic equations required for an analysis of the data may then be written as

$$\log(\eta_0 DM_w/k_BT) = \log f_D(\lambda L) + \log M_L - 0.975 \quad (14)$$

along with eq 11. Thus, in this case, the quantities M_L and $\lambda^{-1}M_L$ may be estimated from a best fit of double-logarithmic plots of the theoretical f_D against λL for properly chosen values of $\lambda^{-1}\kappa_0$, $\lambda^{-1}\tau_0$, and λd_b to that of the observed $\eta_0 DM_w/k_BT$ against M_w, so that we may in principle determine $\lambda^{-1}\kappa_0$, $\lambda^{-1}\tau_0$, λ^{-1}, M_L, and d_b. In this case, however, it is diffiult to determine all five of these parameters by the above curve fitting, since the experimental double-logarithmic plot of $\eta_0 DM_w/k_BT$ against M_w follows its asymptotic straight line of slope $^1/_2$ except for very small M_w, as seen from Figure 4. For simplicity, therefore, we assume that $\lambda^{-1}\kappa_0$ and $\lambda^{-1}\tau_0$ are the same as those determined above from $[\eta]$, and determine the remaining three parameters λ^{-1}, M_L, and d_b.

In Figure 6, the present data (unfilled circles) for $\eta_0 DM_w/k_BT$ (in cm^{-1}) for i-PMMA in acetonitrile at 28.0 °C are double-logarithmically plotted against M_w, and the solid curve for them represents the best-fit theoretical values calculated for $N \geq 2$ from eq 12 with $\lambda d_b = 0.05$, $\log M_L = 1.255$, and $\log(\lambda^{-1}M_L) = 2.747$, the dashed line segment connecting those values for $N = 1$ and 2. The agreement between theory and experiment is seen to be good as in the case of $[\eta]$. The values of the HW model parameters thus determined are listed in the second row of Table 4. The value 45.5 Å of λ^{-1} determined from D is larger than those determined from $[\eta]$ and $\langle S^2\rangle$, while the value 33.0 Å^{-1} of M_L determined from D is smaller than that determined from $[\eta]$ and nearly equal to that determined from $\langle S^2\rangle$. This tendency is the same as that in the case of a-PMMA, for which the values of the model parameters determined from $[\eta]$, D, and $\langle S^2\rangle$ are reproduced in the fourth through sixth rows, respectively, in Table 4, and we note that it is also recognized in the cases of atactic polystyrene[11] and poly(dimethylsiloxane).[16] As mentioned in the previous paper on a-PMMA,[6] it may be regarded as arising from the disagreement between the theoretical and experimental values of Φ_∞ (mentioned above) and ϱ_∞.[15] Considering these facts, it may be concluded that the HW theory may explain rather consistently the three properties $\langle S^2\rangle$, $[\eta]$, and D.

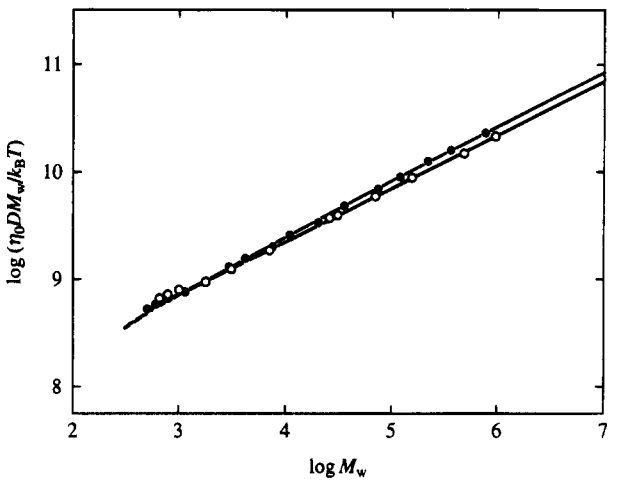

Figure 6. Double-logarithmic plots of $\eta_0 DM_w/k_BT$ (in cm^{-1}) against M_w for PMMA in acetonitrile: (○) present data for i-PMMA at 28.0 °C; (●) previous data for a-PMMA at 44.0 °C.[6] The solid curves represent the respective best-fit HW theoretical values for $N \geq 2$, with the dashed line segments connecting the respective values for $N = 1$ and 2.

Comparison with a-PMMA. We make a comparison of the present results for $[\eta]$ and D for the unperturbed i-PMMA chain with those previously obtained for the unperturbed a-PMMA chain.[5,6] In Figures 5 and 6, the filled circles represent the experimental values[5,6] of $[\eta]$ and $\eta_0 DM_w/k_BT$, respectively, for the latter in acetonitrile at 44.0 °C (Θ), and the solid curves for them represent the respective best-fit HW theoretical values calculated for $N \geq 2$ from eqs 6 and 12 with the values of the HW model parameters given in the fourth row of Table 4 for $[\eta]$ and with those given in the fifth row for $\eta_0 DM_w/k_BT$, each dashed line segment connecting the corresponding theoretical values for $N = 1$ and 2.

The data points for i- and a-PMMAs are seen to agree well with each other for $M_w \lesssim 2 \times 10^3$, although the values of $\eta_0 DM_w/k_BT$ for i-PMMA are there somewhat larger than those for a-PMMA. This agreement is consistent with the previous finding that the values of $\langle S^2\rangle/x_w$ for the two PMMAs are rather close to each other for very small x_w.[1] As M_w is increased, the data points

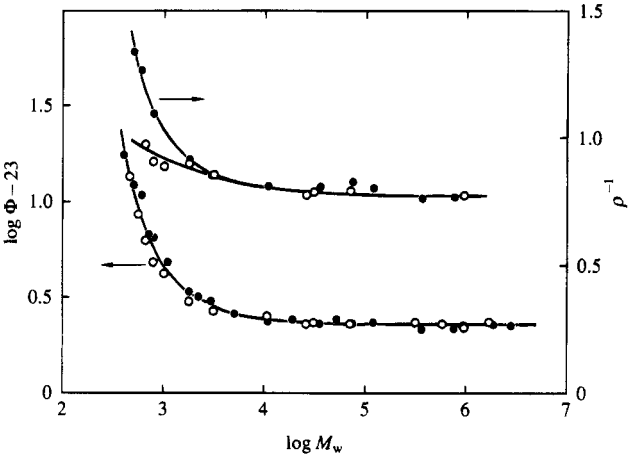

Figure 7. Double-logarithmic and semilogarithmic plots of Φ (in mol^{-1}) and ϱ^{-1} against M_w for PMMA in acetonitrile: (○) present data for i-PMMA at 28.0 °C; (●) previous data for a-PMMA at 44.0 °C.[3,5,6] The solid curves connect the data points smoothly.

for a-PMMA in Figures 5 and 6 deviate downward and upward, respectively, from those for i-PMMA, but both come to follow the respective straight lines of slope $^1/_2$, as seen from Figures 2 and 4, Figure 3 of ref 5, and Figure 5 of ref 6. These deviations correspond to the fact that $\langle S^2\rangle/x_w$ for a-PMMA becomes smaller than that for i-PMMA for $M_w \gtrsim 3 \times 10^3$.[1] It is seen from Figure 5 and 6 that the HW model may explain well the differences in the behavior of $[\eta]$ and D between i- and a-PMMAs, although the agreement between theory and experiment is not very good in the case of $[\eta]$ for a-PMMA.

Finally, we examine the dependences of Φ and ϱ^{-1} on M_w for the two PMMAs. Note that we consider here ϱ^{-1} instead of ϱ itself since the former is just the "reduced hydrodynamic radius" and more suitable for a comparison with the "reduced (molar) hydrodynamic volume" Φ. In Figure 7, the values of Φ (in mol^{-1}) and ϱ^{-1} calculated with the values of $[\eta]$, D, and $\langle S^2\rangle$ for i-PMMA in acetonitrile at 28.0 °C (unfilled circles) and a-PMMA in acetonitrile at 44.0 °C (filled circles) are double-logarithmically and semilogarithmically plotted against M_w, and the solid curves connect the data points smoothly. It is seen that as M_w is increased, both quantities first decrease for $M_w \lesssim 10^4$ and then become independent of M_w for larger M_w.

It is also interesting to see that the values of Φ for the two PMMAs are almost identical with each other (on the ordinate scale displayed) over the whole range of M_w examined. Precisely, the asymptotic (coil-limiting) value Φ_∞ for i-PMMA (in the limit of $M_w \to \infty$) is estimated to be 2.29×10^{23} mol^{-1} as the mean of the five values for the samples iMMcx with $x = 30$, 60, 90, 100, and 170, and it is somewhat larger than the value 2.16×10^{23} mol^{-1} for a-PMMA, which is the mean of the two values for Mr4 and Mr8 given in Table III of ref 15. For a quantitative discussion of Φ_∞, however, proper polydispersity corrections should be made as before,[15] since the molecular weight distributions are somewhat broader for the i-PMMA samples than for the a-PMMA samples. If we assume that the ratio of the z-average molecular weight M_z to M_w is approximately equal to M_w/M_n and that $M_w^{1/2}/(M^{1/2})_w = 1.01$ with $(M^{1/2})_w$ the weight average of $M^{1/2}$ (see Table I of ref 15), then we have $(2.58 \pm 0.11) \times 10^{23}$ mol^{-1} as the corrected value of Φ_∞ for i-PMMA, which is appreciably larger than the corresponding value 2.34×10^{23} mol^{-1} previously[15] estimated for a-PMMA.

In contrast to the rather good agreement above between the values of Φ for the two PMMAs, ϱ^{-1} is appreciably smaller for i-PMMA than for a-PMMA for $M_w \lesssim 2 \times 10^2$. The corrected asymptotic value ϱ_∞ for i-PMMA is estimated to be 1.25 ± 0.01 as the mean of the two values for the samples iMMc16 and iMMc90, and it is slightly smaller than the corresponding value 1.29 ± 0.02 previously[15] estimated for a-PMMA.

Conclusion

For i-PMMA with $f_r \simeq 0.01$ in acetonitrile at 28.0 °C (Θ), it has been found that $[\eta]$ is proportional to $M_w^{1/2}$ for $M_w \gtrsim 5 \times 10^4$ and its deviation from this asymptotic behavior is small even for smaller M_w, while D is inversely proportional to $M_w^{1/2}$ except for $M_w \lesssim 2 \times 10^3$. This is the result expected from the behavior of its $\langle S^2\rangle/x_w$ previously[1] studied. It is interesting to find that even such apparent Gaussian behavior of these steady-state transport coefficients over a wide range of M_w may be well explained by the HW theories with the values of the basic model parameters consistent with those previously determined from $\langle S^2\rangle$.[1] These present results along with those in the previous study of the scattering function[2] confirm the previous conclusion[1] concerning the dependence on f_r of the chain stiffness and local chain conformation of PMMA mentioned in the Introduction. It is however important to emphasize that the above simple dependences on M_w of the transport coefficients in the unperturbed state, i.e., $[\eta] \propto M_w^{1/2}$ and $D \propto M_w^{-1/2}$ except for small M_w do not necessarily mean that the Gaussian chain model is good enough to describe the chain conformation of such a polymer.

On the basis of the present and previous results in the unperturbed state, we proceed to make a study of excluded-volume effects for i-PMMA in dilute solution in the following and forthcoming papers.

References and Notes

(1) Kamijo, M.; Sawatari, N.; Konishi, T.; Yoshizaki, T.; Yamakawa, H. *Macromolecules* **1994**, *27*, 5697.
(2) Horita, K.; Yoshizaki, T.; Hayashi, H.; Yamakawa, H. *Macromolecules* **1994**, *27*, 6492.
(3) Tamai, Y.; Konishi, T.; Einaga, Y.; Fujii, M.; Yamakawa, H. *Macromolecules* **1990**, *23*, 4067.
(4) Yoshizaki, T.; Hayashi, H.; Yamakawa, H. *Macromolecules* **1993**, *26*, 4037.
(5) Fujii, Y.; Tamai, Y.; Konishi, T.; Yamakawa, H. *Macromolecules* **1991**, *24*, 1608.
(6) Dehara, K.; Yoshizaki, T.; Yamakawa, H. *Macromolecules* **1993**, *26*, 5137.
(7) Yamakawa, H. *Annu. Rev. Phys. Chem.* **1984**, *35*, 23.
(8) Yamakawa, H. In *Molecular Conformation and Dynamics of Macromolecules in Condensed Systems*; Nagasawa, M., Ed.; Elsevier: Amsterdam, 1988; p 21.
(9) Yamakawa, H.; Shimada, J.; Fujii, M. *J. Chem. Phys.* **1978**, *68*, 2140.
(10) Yoshizaki, T.; Nitta, I.; Yamakawa, H. *Macromolecules* **1988**, *21*, 165.
(11) Yamada, T.; Yoshizaki, T.; Yamakawa, H. *Macromolecules* **1992**, *25*, 377.
(12) Ute, K.; Asada, T.; Miyatake, N.; Hatada, K. *Makromol. Chem., Macromol. Symp.* **1993**, *67*, 147.
(13) Rubingh, D. N.; Yu, H. *Macromolecules* **1976**, *9*, 681.
(14) Berry, G. C. *J. Chem. Phys.* **1966**, *44*, 4550.
(15) Konishi, T.; Yoshizaki, T.; Yamakawa, H. *Macromolecules* **1991**, *24*, 5614.
(16) Yamada, T.; Koyama, H.; Yoshizaki, T.; Einaga, Y.; Yamakawa, H. *Macromolecules* **1993**, *26*, 2566.
(17) Krause, S.; Cohn-Ginsberg, E. *J. Phys. Chem.* **1963**, *67*, 1479.
(18) Yamakawa, H.; Yoshizaki, T. *J. Chem. Phys.* **1983**, *78*, 572.
(19) Yamakawa, H. *Modern Theory of Polymer Solutions*; Harper & Row: New York, 1971.

MA941159X